Paper

Int'l J. of Aeronautical & Space Sci. 17(2), 139–148 (2016)
DOI: http://dx.doi.org/10.5139/IJASS.2016.17.2.139

IJASS
International Journal of Aeronautical and Space Sciences

Investigation of passive flow control on the bluff body with moving-belt experiment

Joo-Hyun Rho*

High Speed Train Development Team, R&D center, Hyundai Rotem Company, Uiwang 16082, Republic of Korea

Dongho Lee**

Dept. of Mechanical & Aerospace Engineering, Seoul Nat. Univ, Seoul 08826, Republic of Korea

Kyuhong Kim***

Dept. of Mechanical & Aerospace Engineering/Institute of Advanced Aerospace Technology, Seoul Nat. Univ, Seoul 08826, Republic of Korea

Abstract

The passive control methods such as horizontal and vertical fences on the lower surface of the bluff body were applied to suppress the vortex shedding and enhance the aerodynamic stability of flow. For investigating the effects of the passive control methods, wind tunnel experiments on the unsteady flow field around a bluff body near a moving ground were performed. The boundary layer and velocity profiles were measured by the Hot Wire Anemometer (HWA) system and the vortex shedding patterns and flow structures in a wake region were visualized via the Particle Image Velocimetry (PIV) system. Also, it is a measuring on moving ground condition that the experimental values of the critical gap distances, Strouhal numbers and aerodynamic force FFT analyses. Through the experiments, we found that the momentum supply due to moving ground caused the vortex shedding at the lower critical gap distance rather than that of fixed ground. The horizontal and vertical fences increase the critical gap distance and it can suppress the vortex shedding. Consequently, the stability characteristics of the bluff body near a moving ground could be effectively enhanced by the simple passive control such as the vertical fences

Key words: Passive flow control, Moving belt experiment, Vortex shedding

1. Introduction

Numerous studies have been done on the unsteady flow features around a bluff body due to vortex-induced oscillations because they provide fundamental information related to a large number of engineering problems. The vortex around a bluff body leads to unsteady oscillations of aerodynamic features, which result in sudden aerodynamic and structural instability. The suppression or control of vortex shedding is crucial for improving the safety, stability and reducing aerodynamic force of bluff body. The unsteady flow fields around bluff bodies are dominated by flow separation, reattachment, and unsteady vortex formation in the wake region[1]. As bluff bodies approach the ground, vortex shedding becomes suppressed and dependent on various parameters such as the Reynolds number, the breadth-to-height ratio (B/D), the blockage ratio, the free-stream turbulence intensity and the incoming turbulent wall boundary layer thickness, etc.[2]

To examine the flow phenomena around bluff bodies near a ground, various experimental researches have been performed. For examples, the flow patterns around a cylinder near ground have been investigated by Okajima[3], Lyn[4], Bosch[5], Bailey[6], Martinuzzi[7], etc. Also, many

* Ph. D
** Professor
*** Professor, Corresponding author: aerocfd1@snu.ac.kr

Received: May 22, 2015 Revised: April 8, 2016 Accepted: June 13, 2016

http://ijass.org pISSN: 2093-274x eISSN: 2093-2480

studies have been performed to analyze the characteristics of vortex shedding formation and various control methods, which suppress vortex shedding and reduce aerodynamic drag. Tamura[8] studied the averaged and fluctuating statistics of lift and drag acting on a square sectioned cylinder with sharp, chamfered and rounded corners. With these controlled shapes of a square cylinder, the shear layers became close to the side surface. Accordingly reattachment was enhanced and drag forces were reduced. Duell et al.[9] experimentally investigated the effect of a mounted cavity in the base region. They reported that the mean base pressure was increased about 4% and 11% when the ratio of depth and height (D/H) was 0.2 and 0.8, respectively. The recirculation length was increased by 1.6~1.8 times the base recirculation length. Choi and Kwon[10] studied the physical mechanism of aerodynamic and aero-elastic instability of a bluff body with various corner cuts and attack angles. They claimed that the corner cut method produced better behavior for aerodynamic characteristics but could not suppress the vortex shedding. Khalighi[11] reported that the presence of the plates in the wake region reduces the intensity of the recirculation velocity of the base region, which, in turn, reduces the vortex shedding and the unsteadiness of the wake, and increases the pressure at the base region. B.S. Lee [12] and T.Y. Kim [13] reported that the passive control methods in which vertical and horizontal fences are attached in the lower surface of the cylinder could suppress the vortex shedding past a cylinder. Also, the flow patterns around bluff bodies placed near a moving ground have been studied extensively. Arnal et al.[14] performed a numerical simulation of a square cylinder under the condition of the free-stream and fixed and sliding wall conditions according to the Reynolds number. Kumarasamy and Barlow[15] studied the flow over a half-cylinder close to a moving wall and reported that the Strouhal number did not change but the drag greatly deviated from the stationary wall. Kim and Geropp[16] investigated the flow around some two-dimensional bluff bodies by wind tunnel experiments equipped by a moving-belt. They showed that lift forces increased wakes lengthened with decreasing clearance. Bhattacharyya and Maiti[17] performed a numerical simulation of a square cylinder placed in a moving ground under Re=1,000. The results showed that the averaged drag experienced by the moving ground was higher than that of the corresponding stationary case.

Numerous studies have provided little information of the flow features on a bluff body near a moving ground in the turbulent Reynolds number region. T.Y. Kim [18] performed a numerical simulation of a square cylinder with a passive control placed in the moving ground. Therefore, the objective of this study is to provide additional information of the flow-field around a bluff body on a moving ground by the experiment as well as on stationary ground with gap distances. Based on this investigation, we will discuss the effects of passive control such as the horizontal and vertical fences near a moving ground in the enhancement of aerodynamic stability.

2. Experimental Apparatus and Flow Conditions

Experiments were carried out in the low turbulence subsonic wind tunnel at the Institute of Fluid Science in Tohoku University. This wind tunnel system uses a moving-belt system to simulate ground effect, and the working section can be changed from closed type to open-jet type. The free-stream turbulence level in the open circuit at flow velocity of 15 m/s was found to be about 0.07 % of the free-stream velocity.

Figure 1 shows the experimental apparatus. The inflow velocity was measured by the Pitot-static tube mounted at the upper position of the test section. The mean velocity and the turbulent field around the square cylinder were measured using an I-type hot-wire and CTA.

The averaged aerodynamic lift and drag were measured by the 3-axis load-cell connected to both ends of the experimental models. The sampling frequency was 1 kHz, and the data from the two load-cells were added for 30 seconds. These unsteady data from the load-cell were used to capture the shedding frequency via the Fast Fourier Transform (FFT). For flow visualization, the two-component Particle Image Velocimetry (PIV) as the laser light-sheet visualization technique with a smoke-tracer was employed to observe the dynamic behavior of the flow.

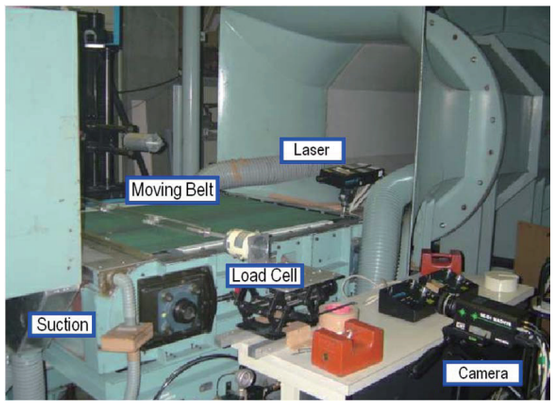

Fig. 1. Experimental apparatus at IFS in Tohoku University

DOI: http://dx.doi.org/10.5139/IJASS.2016.17.2.139

The average inflow velocity was set to u^{∞}=10 m/s, and hence Re=20,000 (based on the inflow velocity, u∞, and the cylinder height, D). For the sharp edged bluff body, although the Reynolds number increases from 2×10^4 to 2.5×10^5, the drag coefficient of the square cylinder changes little because the separation point does not move and a vortex is still generated in high Reynolds number regions. [20] [21] Therefore, it is reasonable that the results of the general square cylinder at the Reynolds number of 20,000 would still be remained valid in the real condition.

Figure 2 shows side view about the layout of the experimental apparatus and the coordinate system. The test model was a two-dimensional square cylinder, made of acryl to ensure sharp edges, with height D=30 mm and length L=800 mm, and hence, span of 26.7D, resulting in a blockage ratio of approximately 3%. Also the lengths of the horizontal and vertical fences were 0.1D (3 mm), and the thickness was 0.07D (2.1 mm), as shown in Fig. 3(c), (d). The experimental models were mounted by two load-cells horizontally, and the gap distances at X=235 mm downstream were controlled by a 1-axis traverse system, as shown in Fig. 1.

3. Results and Discussion

To verify the vortex shedding and flow structure for different ground conditions and gap distances, various experimental approaches and results, i.e. velocity profiles, spectral analysis, flow visualization, were considered. Throughout these experimental analyses, we analyzed the vortex shedding around a bluff body and investigated the effects of passive control devices on the enhancement of the aerodynamic stability of the square cylinder. The experiments performed in this research and the result associated with each experiment is as followed.

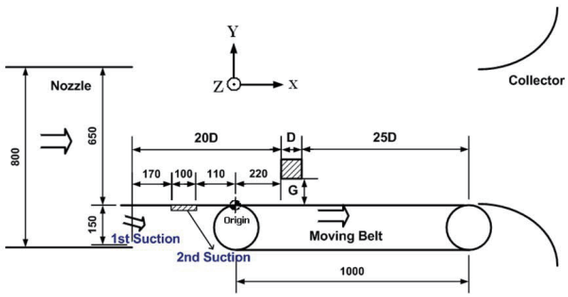

Fig. 2. Layout of the experimental apparatus

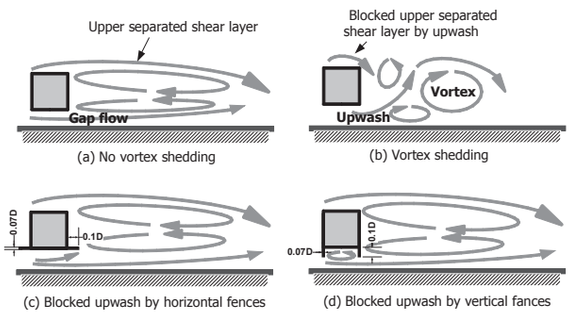

Fig. 3. Schematic diagrams of vortex shedding mechanism and controlled shapes (18)

3.1 Velocity survey over the moving-belt

Figure 4 shows the distribution of time-mean streamwise velocity in the transverse direction at different lateral positions, Z=200, 0, -200 mm, at the locations X=250 mm. (Here, the origin point is shown in Fig.2.) Boundary layer was measured for the following three cases: fixed ground – without suction and moving-belt; suction ground – only operates the 1st and 2nd suction system without moving-belt; and moving ground – with both suction system and moving-belt system. For controlling the boundary layer thickness and reproducing the turbulent flow, the trip wires were mounted at the nozzle of the wind tunnel. On the fixed ground, the boundary layer thickness at the position Z=0 mm was about 60 mm, however at Z=200 and -200 mm, it is about 25 mm. This difference was due to the suction system, which was installed to eliminate the incoming boundary layer induced by the wind tunnel, and the open test section

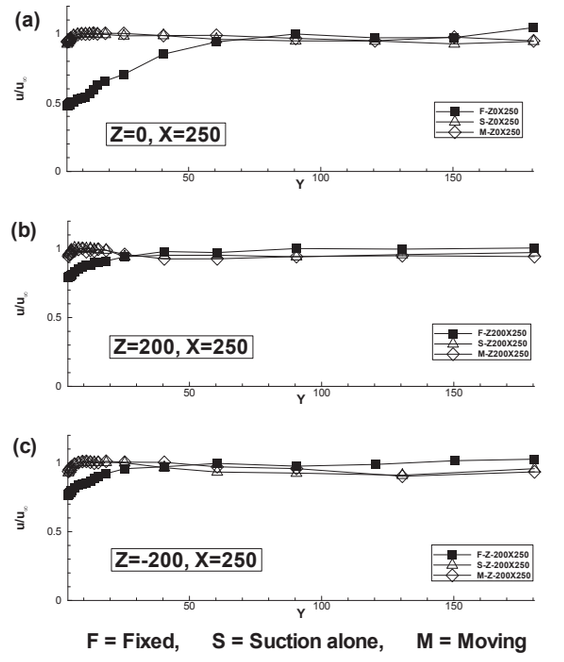

Fig. 4. Boundary layer along the Z-direction

used for installing moving-belt system.

At the open test section, the flow at the edge side of the test section diverged; however, the boundary layer thickness in the suction and moving case was about 3 mm at all positions. Therefore, the moving-belt system effectively simulated the ground effects. The distribution of the mean velocity along the centerline, that is, Z=0 mm, at different streamwise positions, X=100, 250, 400 mm, are shown in Fig. 5. (Here, the origin point is shown in Fig. 2.) As expected, the velocity deficit near the ground is minimized when the moving-belt is running and the suction is operated. There is no difference between the suction alone and moving belt cases at X=100 mm because of location of the suction system. However, as the x-directional distance increases, the effect of the suction alone becomes weak and the boundary layer thickness is about 5 mm at X=250 mm, and 10 mm at X=400 mm. On the other hand, the moving belt system showed the consistent performance of the boundary layer elimination on the entire test region even if the boundary layer slightly increased with the increase of the x-directional distance. The boundary layer thickness increases only slightly because the belt imparts momentum to the near adjacent flow and its vibration increases the turbulence intensity.

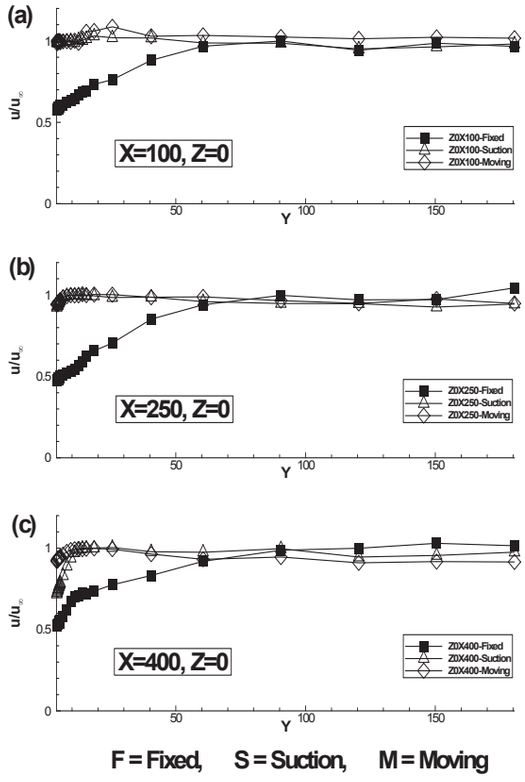

Fig. 5. Boundary layer along the X-direction

3.2. Averaged velocity in wake region

Figure 6 shows the y-directional velocity profiles along the streamwise position at G/D=1.0 for various ground conditions. When the suction or moving belt condition is applied at x/D=0 (X=250 mm), more momentum is supplied from the gap region to the wake region. Because the velocity in the wake region is higher than that of the fixed ground, the pressure loss produces an aerodynamic drag. As x/D increases from 0 to 1, 3, 5 (X=250 to 280, 340, 400 mm), the velocity profile for the fixed ground and that for moving and suction ground becomes slightly different. The reversed flow in the wake region is weak and recovered to the free-stream.

Figure 7 shows the velocity profiles of the baseline shape at G/D=0.3, 0.6, 0.8 and 1.0. At G/D=0.3, where the vortex shedding is suppressed in all ground conditions, the flow pattern is similar to each other except in the gap region.

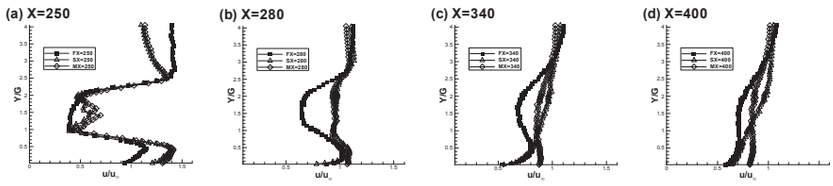

Fig. 6. Mean velocity at G/D=1.0 along the x-direction (F: Fixed, S: Suction alone, M: Moving)

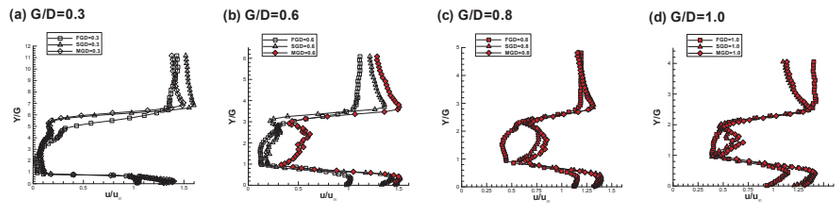

Fig. 7. Mean velocity on the base shape at X/D=0

DOI: http://dx.doi.org/10.5139/IJASS.2016.17.2.139

However, at G/D=0.6 and 0.8, where there is intermittent vortex shedding according to the ground conditions, the difference of velocity profiles in both the gap and the wake region is significant, and this difference has a strong influence on the vortex shedding mechanism. At G/D=1.0, where the regular vortex shedding is established, the flow pattern is similar to each other except in the gap region due to effects on the boundary layer.

The velocity pattern of controlled shapes is shown in Fig. 8. As mentioned in above section, when the vortex shedding is suppressed, the flow pattern of controlled shapes is not different from the flow pattern at the base shape. At G/D=0.8, only vortex shedding occurs if the horizontal fence is mounted on the moving ground, and the velocity profile in wake region is significantly different from those of the other cases.

3.3. Averaged velocity in gap region

Figure 9 shows the time averaged stream wise x-directional velocity distributions measured at the exit region of the gap between the square cylinder and ground according to the various gap distances. In the cases where the vortex shedding occurs, higher momentum is provided to the wake region than in the cases without vortex shedding. Also the position (y/G), where the maximum velocity, $(u/u^{\infty})_{max}$ was measured, can be seen to move closer to the lower surface of the square cylinder. At G/D=0.3 and 0.6 on the fixed ground, the averaged velocity is lower than those of the other cases at G/D=1.0 and 1.5, where the regular vortex shedding occurs. The moving ground cases, in Fig. 9(e), have a similar velocity profile as the fixed ground cases, except the supplemental momentum due to the absence of the separated shear layer on the ground. These experimental results are similar to those of the numerical simulations (X).

In the cases of horizontal fences near a fixed ground in Fig. 9(b), the gap velocity is more interfered and canceled by viscous effects from the ground, and hence, the vortex shedding happens at G/D=1.5 only. But, only a little effect is observed in the moving ground as shown in Fig. 9(d) and vortex shedding occurs at G/D>0.8. The velocity profiles with the installation of the vertical fences are shown in Fig. 9(c), (f). In these Figure, the vertical fences diminish the momentum supplement to the wake region and suppress the vortex shedding.

3.4. Spectral Analysis

The 3-axis load-cell which is located beside the experimental model was used for the measurement of the

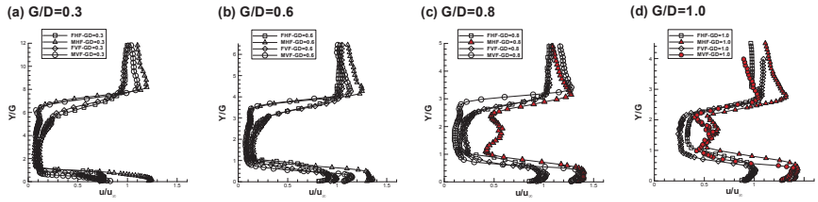

Fig. 8. Mean velocity on controlled shapes at X/D=0 (HF: Horizontal fences, VF: Vertical fences)

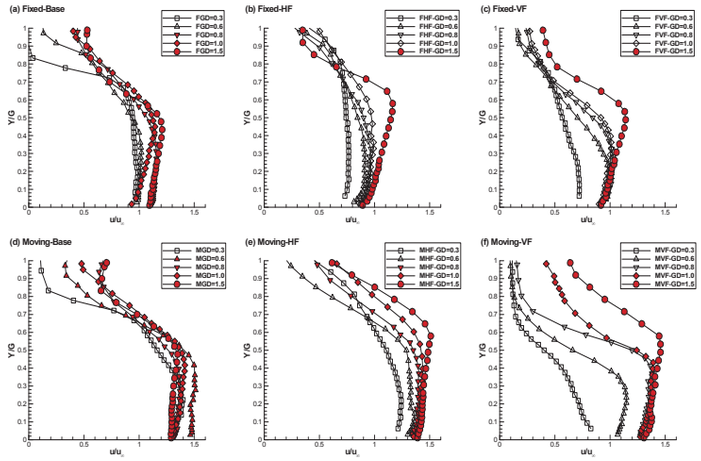

Fig. 9. Mean velocity profile in gap region on the fixed and the moving ground(□ △ ◇▽○ : Vortex suppressed, ■▲◆▼● : Vortex shedding)

shedding frequency. The data was measured for one minute with the 100 Hz sampling rate. The dominant – single and sharp spectral peak – shedding frequency, fs in the frequency spectrum was calculated by FFT analysis then, the Strouhal number, St was calculated from Eq. (1).

$$St = \frac{Df_s}{U_\infty} \tag{1}$$

Figure 10 shows the Strouhal number distributions of the base shape according to the ground conditions and change of the critical gap distances. In the case of the suction and the moving belt, the critical gap distance is found at G/D=0.5, but on fixed ground at G/D=0.7. The Strouhal number for the suction and the moving belt is higher than that for the fixed ground because of the absence of the separated shear layer on the ground. At G/D=0.6 in the case of the suction and the moving belt, the Strouhal number with the peak value about St=0.14 is converged to St=0.135. When the square cylinder locates at G/D<1.2 on the fixed ground, the regular vortex shedding is still affected by the separated shear layer on the ground. However, as the gap distance increases, the ground effect is weakened and the distribution of the Strouhal number has a similar pattern to that of the suction and the moving belt case at G/D>1.5. The numerical results (18) have shown that the critical gap distance exists near G/D=0.35 for the moving ground and at G/D=0.55 for the fixed ground. However, according to the results of present experiments, the values of the critical gap distance are different from those of the numerical results; this difference results from the 3-D effect induced by the side flow on the test section. Undoubtedly, the flow at the centerline of the test model has been confirmed as a two-dimensional flow by hot-wire experiment.

Figure 11 shows the critical Strouhal number gap distance associated to the control devices. The shape with the vertical fences has a lower Strouhal number than with the horizontal fences. In the case of the horizontal fences, the critical gap distance slightly increases about 0.1D from the baseline on the suction and the moving belt. On the other hand, the vertical fences increase the critical gap distance about 0.5D via the suppression of the vortex shedding. For the fixed ground, the only vortex shedding is observed at G/D=1.5 in both passive controlled shapes.

Figure 12~14 show the power spectrum by FFT analysis according to the ground conditions and the passive flow control. In these Figures, the peak frequency, which was captured near 15 Hz and 30 Hz, is regarded as the noise generated by the operation of the wind tunnel with model. In addition to the FFT analysis of aerodynamic forces could be use a simple method to know the vibration motion of bluff body.

In the fixed ground, the dominant frequency is not found at G/D=0.4 and 0.6; however, it is observed at G/D>0.8. The

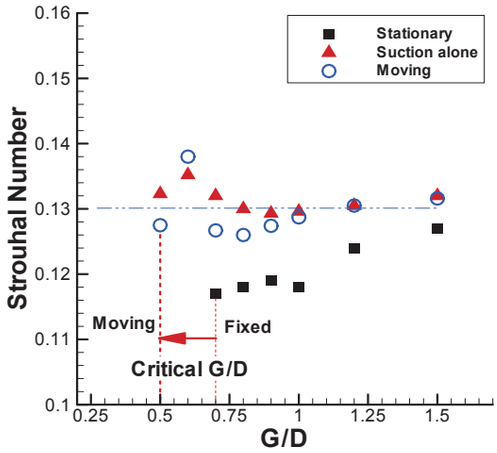

Fig. 10. Strouhal number of the base shape

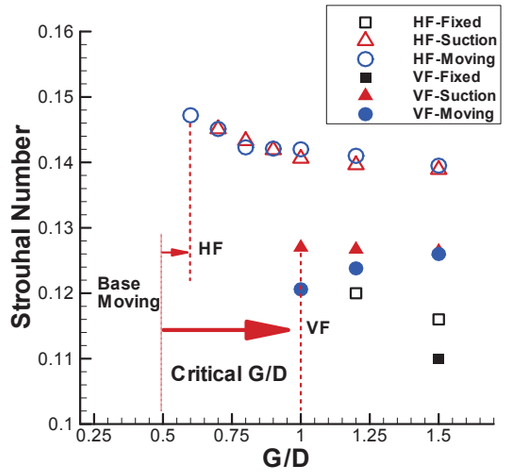

Fig. 11. Strouhal number of controlled shapes

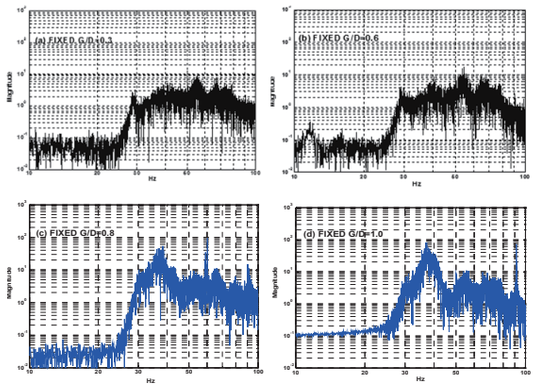

Fig. 12. FFT analysis of the base shape at the fixed ground

DOI: http://dx.doi.org/10.5139/IJASS.2016.17.2.139

amplitude of the peak frequency on the fixed ground is smaller than those of other periodic vortex shedding cases for the moving ground. That is because the moving ground helps the vortex shedding behind a square cylinder. The regular vortex shedding can be observed at the G/D>0.6 on the moving ground, as shown in Fig. 13. When the passive control devices such as horizontal and vertical fences are installed on the square cylinder, the vortex shedding is suppressed effectively, especially with the vertical fence, as shown in Fig. 14.

In the present research, statistical analysis of uncertainty was performed to determine the accuracy of the experimental results. The uncertainty analysis established by the standard of ISO was applied. Every uncertainty was calculated by using this method. In the unsteady flow analysis, the major source of error came from the data scattering during measurements. The longer sampling time could minimize the uncertainties of the shedding frequency and aerodynamic coefficients. That is, because the uncertainty of the free stream velocity was 0.5% in the present research, the use of large sampling time could minimize the uncertainty to less than ±0.001 in the gap flow region. The Strouhal number had the uncertainty of ±0.003

3.5. Aerodynamic characteristics

Figure 15 shows the coefficients of the aerodynamic drag and lift according to G/D. The drag coefficients of the moving ground cases are higher than those of the cases on the fixed ground. In the fixed ground cases, the drag coefficient does not vary with the change of gap distance, but the drag on the moving ground has the peak value around G/D=0.8. The lift has a negative value due to the pressure drops induced by the accelerated flow in the gap region. However, the lift on the moving ground has the minimum value at G/D=0.5, and then increases as the gap distance increases. For investigating the

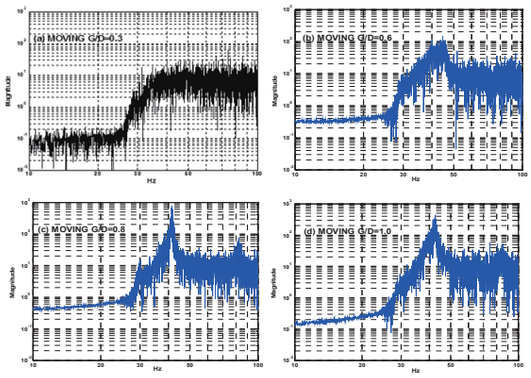

Fig. 13. FFT analysis of the base shape at the moving ground

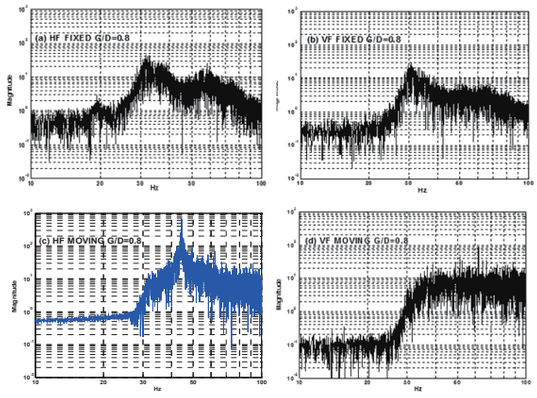

Fig. 14. FFT analysis on controlled shapes at G/D=0.8

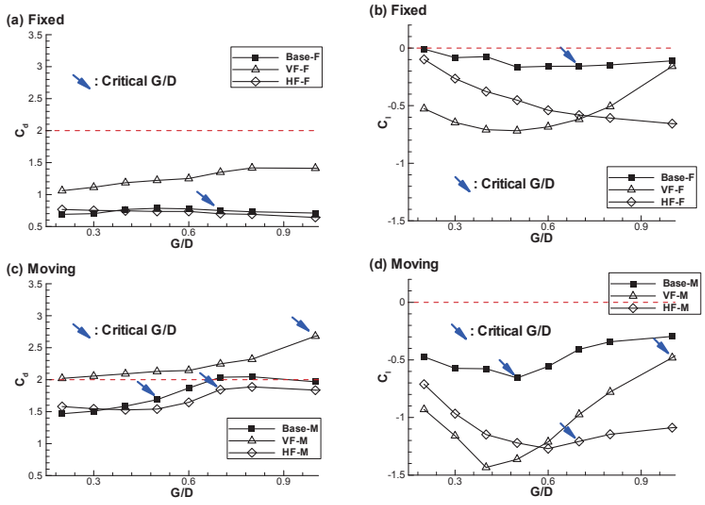

Fig. 15. Aerodynamic coefficient of controlled shapes according to ground conditions

effects of the ground conditions and the passive flow control, drag and lift coefficients of the baseline and controlled shapes are compared in Fig. 15. The suction and the moving belt cause the aerodynamic drag to increase abruptly because the pressure recovery in the wake region decreases due to the sufficient momentum supply from the gap region, as shown in Fig. 15(a), (c). Fig 15(b), (d) explains the lift coefficients for various gap distances. At G/D<0.7, there is a large difference of lift, but under that height, the value of the lift are similar in all ground conditions. This pattern has nothing to do with the experimental models. In the cases of the controlled shape obtained from application of vertical fences, the minimum value of lift exists around G/D=0.4. Also in these Figures, the horizontal fences in the fixed ground condition enlarge the domain where the lower separated shear layer is canceled by the opposite separated shear layer on the ground, and finally it can suppress the vortex shedding.

But, in the moving ground case, the boundary layer on the ground is not strong enough to suppress the vortex shedding behind the square cylinder. On the other hand, the vertical fence can suppress the vortex shedding efficiently in all ground conditions due to the decrement of effect of gap distance. However, the drag increases because the vertical fence is mounted perpendicular to the flow direction, and hence raises the aerodynamic drag.

3.6. Flow visualization by PIV system

The flow visualization experiments by PIV system were performed to confirm the flow pattern and vortex structure past a square cylinder. In general, the PIV system can measure quantitative data, but the present experimental results were only used for the flow visualization because of the performance limitation of the PIV system used in this experiment.

The PIV experiments were performed under the following condition: sampling frequency was 15 Hz, and a total of 100 pictures were captured by the 1K X 1K pixel CCD camera continuously. The laser was installed at the collector of the wind tunnel, and the CCD camera was positioned perpendicular to the laser.

Figure 16~18 show the flow behavior behind the square cylinder at G/D=0.3, 0.6 and 0.8 on the fixed and moving ground conditions. At G/D=0.3, vortex shedding is suppressed in both ground conditions without the interaction between the lower and upper separated shear layers. Especially the gap flow between the square cylinder and the ground is squeezed as jet flow without roll up behind the square cylinder. However, at G/D=0.6, the flow structure is distinctly different according to the ground condition. In a moving ground, there is regular vortex shedding, as shown in Fig. 17, because the velocity is higher in the wake region than in the fixed ground cases. As the gap distance increases, the ground effect becomes weak and the vortex shedding occurs for both ground conditions, as shown in Fig. 18. Fig. 19 and 20 show the flow pattern induced by the horizontal and vertical fences at G/D=0.8 respectively. In the case of the controlled

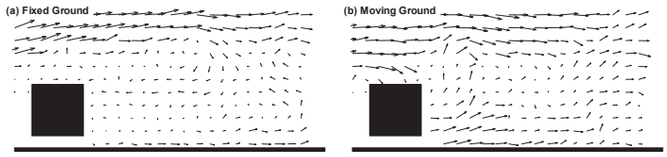

Fig. 16. Flow visualization by PIV on the base shape at G/D=0.3

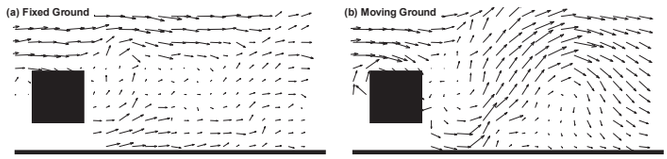

Fig. 17. Flow visualization by PIV on the base shape at G/D=0.6

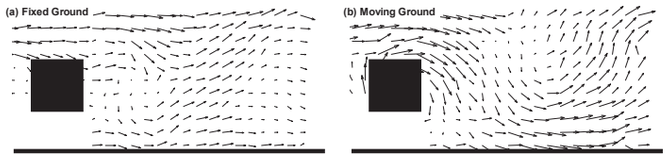

Fig. 18. Flow visualization by PIV on the base shape at G/D=0.8

DOI: http://dx.doi.org/10.5139/IJASS.2016.17.2.139

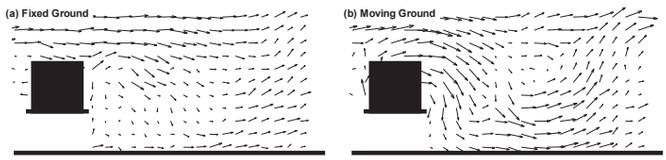

Fig. 19. Flow visualization by PIV on horizontal fences at G/D=0.8

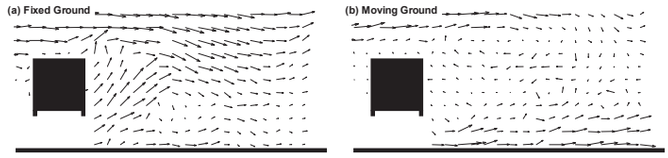

Fig. 20. Flow visualization by PIV on vertical fences at G/D=0.8

shape obtained with the application of horizontal fences as shown in Fig. 19, vortex shedding is suppressed on the fixed ground, but not on the moving ground. However, the controlled shape obtained with the application with vertical fences has no vortex shedding on both ground conditions as shown in Fig. 20.

4. Conclusion

The passive flow control devices such as horizontal and vertical fences were attached on the lower surface of the bluff body and the unsteady flow features around the bluff body were investigated via wind tunnel experiments with a moving belt system.

The passive flow control for an aerodynamic stability was investigated by wind tunnel test with moving belt technique. It was measured on moving ground condition that the experimental values of the critical gap distances, Strouhal numbers, aerodynamic force FFT analyses and flow visualizations with PIV.

Through the experiments, we found that the momentum supply due to the moving ground condition causes vortex shedding at a lower critical gap distance than that of the fixed ground case.

The passive flow control shows that the vertical fences can suppress the vortex shedding efficiently under both fixed and moving ground conditions, whereas the horizontal fences can suppress the shedding on only the fixed ground. It is because the vertical fences have the similar effects of decreasing the gap distances and increasing momentum dissipation as the horizontal fences. The enhancement of the aerodynamic stability of the bluff body is caused by the suppression of the vortex shedding.

Acknowledgement

This research was supported by a grant (14PRTD-C061723-03) from Technology Advancement Research Program funded by Ministry of Land, Infrastructure and Transport of Korean government and by Space Core Technology Program through the National Research Foundation of Korea(NRF) funded by the Ministry of Science, ICT & Future Planning(NRF-2015M1A3A3A05027630).

References

[1] T. Y. Kim, B. S. Lee, D. H. Lee, , D. H. Lee, A Study on Vortex Shedding Around a Bluff Body Near the Ground, SAE Paper 2003-01-1652., (2003), Detroit.

[2] D.F.G. Durao, P.S.T. Gouveia, J.C.F. Pereira, Velocity characteristics of the flow around a square cross section cylinder placed near a channel wall, Experiments in Fluids, 11, (1991), pp.341-350

[3] Atsushi Okajima, Strohal numbers of Rectangural Cylinders, , J. Fluid Mech.., (1997), pp. 201-237.

[4] Lyn, D. A., Einav, S., Rodi, W., Park, J. H., A Laser-Doppler Velocimetry Study of Ensemble-Averaged Characteristics of the Turbulent near Wake of a Square Cylinder, J. Fluid Mech., 304, (1995), pp. 285-319.

[5] Bosch, G., Kappler, M., Rodi, W., Experiments on the Flow Past a Square Cylinder Placed near a Wall, Exp. Thermal Fluid Sci., 13, (1996), pp. 292-305.

[6] Bailey, S. C. C., Kopp, G. A. and Martinuzzi, R. J., Vortex Shedding form a Square Cylinder near a Wall, J. Turbulence, 003, (2003), pp. 1-18.

[7] Martinuzzi, R. J., Bailey, S. C. C, Kopp, G. A. Influence of Wall Proximity on Vortex Shedding from a Square Cylinder,

Experiments in Fluids, 34, (2003), pp. 585-596.

[8] Tamura, T. and Miyagi, T., The effect of Turbulence on Aerodynamic Forces On a Square Cylinder with Various Corner Shapes, J. Wind Eng. Ind. Aerodyn., 83, (1993), pp. 135-145.

[9] Edward G. Duell and A.R. George, Experimental Study of a Ground Vehicle Body Unsteady Near Wake, SAE Paper 1999-01-0812, (1999).

[10] C. K. Choi, Kwon and D. K., Aerodynamic Stability for Square Cylinder with Various Corner Cuts, Wind and Structure, 2(3), (1999), pp. 173-187.

[11] Khalighi B., S. Zhang and C. Koromilas, Balkanyi, S.R, P. Bernal, G. Laccarino and P. Moin, Experimental and Computational Study of Unsteady Wake Flow Behind a Bluff Body with a Drag Reduction Device, SAE Paper 2001-01-1042, (2001).

[12] B. S. Lee, T. Y. Kim, D. H. Lee, Control of Vortex Shedding behind a Rectangular Cylinder near the Ground, Numerical Heat Transfer, Part A, 47, No 8, (2005), pp. 787-804.

[13] T. Y. Kim, B. S. Lee, D. H. Lee, Study of the Unsteady Wakes Past a Square Cylinder near a Wall, J. Mech. Sci. Tech. 19-5, (2005), pp. 1169-1181.

[14] Arnal, M. P., Goering, D. J., Humphrey, J. A. C, Vortex Shedding From a Bluff Body Adjacent to a Plane Sliding Wall, J. Fluid Eng., 113, (1991), pp. 384-398.

[15] Sanjay Kumarasamy, Jewel B. Barlow, Computation of unsteady flow over a half-cylinder close to a moving wall, J. Wind Eng. Ind. Aerodyn., 69-71, (1997), pp. 239-248.

[16] M. S. Kim and Geropp, D., Experimental Investigation of the Ground Effect on the Flow around Some Two-Dimensional Bluff Bodies with Moving-belt Technique, J. Wind Eng. Ind. Aerodyn., 74-76, (1998), pp. 511-519.

[17] Bhatacharyya, S., Maiti, D. K., Vortex Shedding for Flow over a Square Cylinder Close to a Moving Ground, IUTAM Symposium, New Jergey, USA., (2003).

[18] T. Y. Kim, , B. S. Lee, D. H. Lee, The Enhancement of Aerodynamic Characteristics on Bluff Bodies near a Moving, JSME International Journal, (2006), pp. 787-796.

DOI: http://dx.doi.org/10.5139/IJASS.2016.17.2.139